Assembly, conductivity, and chemical reactivity of sub-monolayer gold nanoparticle junction arrays

ARTICLE *in* SENSORS AND ACTUATORS B CHEMICAL · FEBRUARY 2008

Impact Factor: 4.1 · DOI: 10.1016/j.snb.2007.10.013

5 AUTHORS, INCLUDING:

Sergey N Gordeev
University of Bath
87 PUBLICATIONS **868** CITATIONS

SEE PROFILE

Available online at www.sciencedirect.com
ScienceDirect
Sensors and Actuators B 129 (2008) 947–952
SENSORS AND ACTUATORS B CHEMICAL
www.elsevier.com/locate/snb

Assembly, conductivity, and chemical reactivity of sub-monolayer gold nanoparticle junction arrays

Robert W. French [a], Elizabeth V. Milsom [a], Andriy V. Moskalenko [b], Sergey N. Gordeev [b], Frank Marken [a,*]

[a] *Department of Chemistry, University of Bath, Claverton Down, Bath BA2 7AY, UK*
[b] *Department of Physics, University of Bath, Claverton Down, Bath BA2 7AY, UK*

Received 3 August 2007; received in revised form 3 October 2007; accepted 5 October 2007
Available online 18 October 2007

Abstract

Assemblies of gold nanoparticles (nominal 20 nm in diameter) and poly-(diallyldimethylammonium chloride) (PDDAC) are formed on tin-doped indium oxide (ITO) and glass substrates in a layer-by-layer deposition process. Electron microscopy imaging suggests clustering and sub-monolayer formation even after multiple deposition cycles. Voltammetric characterisation of the gold-PDDAC assemblies demonstrates at low coverage a facile electron transport perpendicular to the film but essentially insulating characteristics laterally across an inter-electrode gap of 40 μm. However, gentle removal of the organic assembly components (PDDAC) in a room temperature UV-ozonolysis process allows the array of "clean" gold–gold junctions to become electrically conducting due to (i) random multiple tunnel junction pathways and (ii) ionic conductivity through a thin water layer. In this room temperature ozone-cleaned state, the gold assembly is considerably more electrically conducting when compared to thermally cleaned films. The crucial effect of humidity on the resistivity and capacitive currents for gold nanoparticle junction arrays is demonstrated. The gold nanoparticle films readily react with thiols and dithiols from the gas phase which results in a dramatic increase in resistivity. The process is fully reversible and the sensor re-usable after UV-ozonolysis cleaning. Measurements are reported for a range of dithiols with different carbon chain lengths demonstrating that tunnel junction effects are likely to be responsible for the electrical conductivity.

Keywords: Assembly; Tunnel junction; Gold nanoparticle; Random arrays; Thiol; Gas; UV; Ozone; Chemiresistor; Sensor

1. Introduction

Nanoparticle arrays assembled in two or three dimensions have attracted interest in several analytical [1,2] and gas sensing [3,4] applications. The formation of these nanoparticle array films is often based on drop-cast [5,6] or the versatile layer-by-layer deposition process [7,8] which allows suitable metal nanoparticles, e.g. gold, to be combined with a suitable binder molecule, e.g. thiols [9] or poly-cationic binders [10], in order to form thin responsive films usually with chemiresistive properties. Very interesting films for solvent vapour sensing based on silk [11] and on dendrimer [12,13] binders have been proposed. Metal ions have been employed to trigger gold nanoparticle assembly processes for thin film chemiresistive sensor applications [14,15]. The study and application of tunnel or molecular junctions (e.g. in crossed wire sensors [16]) has widened over the recent years [17,18] but chemiresistive effects in sensor applications have been investigated predominantly in junction arrays or in nanowire devices [19].

In this study, exploratory work with thin self-assembled films is reported and the formation of a sub-monolayer film of gold nanoparticles bound together with a poly-cationic binder (poly-(diallyldimehtylammonium chloride or PDDAC)) is investigated. It is shown that, when deposited in a layer-by-layer manner, films with clusters of nanoparticles are formed and these clusters are only gradually inter-connected after many deposition cycles. The extremely low electrical conductivity of these sub-monolayer films can be improved after chemical (UV-ozonolysis) removal of the organic (PDDAC) binder components. Films become very sensitive to humidity and to

* Corresponding author.
E-mail address: F.Marken@bath.ac.uk (F. Marken).

0925-4005/$ – see front matter © 2007 Elsevier B.V. All rights reserved.
doi:10.1016/j.snb.2007.10.013

vapours. The response to thiols and dithiols is demonstrated and the re-usability of probes after surface ozonolysis allows the effect of different vapours to be compared quantitatively.

2. Experimental

2.1. Reagents

Chemical reagents such as 70% phosphoric acid, NaOH, KOH, tartaric acid, oxalic acid, hexanethiol, butanethiol, ethylenedithiol, butylenedithiol, octylenedithiol, poly-(diallyldimethylammonium chloride) of very low molecular weight ($M_w < 10^5$, 35 wt.% in water) (all Sigma–Aldrich), gold nanoparticles (Sigma Gold Colloids nominal 20 nm diameter, mean 17–23 nm, monodisperse, approx. 0.01% as $HAuCl_4$ in water) were obtained commercially and used without further purification. Demineralised and filtered water was taken from an Elga purification unit with a resistivity not less than 18 MΩ cm. Pureshield argon (BOC) was employed in controlled atmosphere experiments. If not stated otherwise the temperature during experiments was 22 ± 2 °C and the relative humidity ca. 60%.

2.2. Instrumentation

For electrochemical and conductivity measurements a microAutolab III system (EcoChemie, Netherlands) was employed. In electrochemical experiments a conventional three-electrode cell with platinum counter and saturated Calomel reference (SCE, Radiometer, Copenhagen) were employed. Conductivity measurements were conducted in two-electrode mode. In controlled humidity experiments a HMP50 temperature and relative humidity probe (Campbell Scientific) was employed connected to the external potential input of the microAutolab potentiostat system. The humidity chamber was controlled with water-saturated air and with solid KOH (relative humidity range 10–100% [20]). A tube furnace (Elite, UK) was employed for thermal treatments and a room temperature UV-ozonolysis cleaner (Bioforce, USA) was used for mild chemical cleaning. Room temperature field emission gun scanning electron microscopy (FEGSEM) images were obtained using a Leo 1530 FEGSEM system. Samples were gold sputter coated prior to imaging. Lithography procedures were carried out using standard procedures as described below.

2.3. Lithography of tin-doped indium oxide film electrodes

Tin-doped indium oxide (ITO, 15 Ω/square, Image Optics, Basildon, UK) coated glass slides were washed in ethanol and demineralised water, covered with PRP positive photoresist spray (RS components, UK) and left to dry in the dark for a minimum of 24 h. UV exposure was carried out with a positive electrode mask (see Fig. 1, Vision Graphics, UK) under a UV light source for 20 min. The electrodes were then carefully developed in aqueous 0.175 M NaOH solution at ca. 20 °C leaving a green resist layer on unexposed areas. ITO etching was carried out in 1 wt.% tartaric acid and 3 wt.% oxalic acid solution at 35 °C for approximately 20 min [21]. The photoresist was then removed using acetone, the slides were once again thoroughly rinsed, and then for final cleaning placed into a tube furnace (Elite, UK) for half an hour at 500 °C in air.

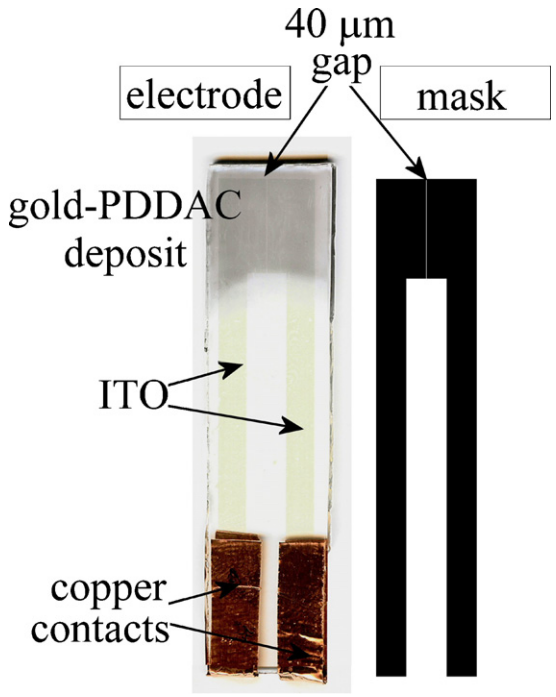

Fig. 1. (A) Photographic image of a gold-PDDAC coated (16 deposition cycles) ITO electrode with a 40 μm inter-electrode gap and copper contacts. (B) Mask used to produce the patterned ITO electrode in a lithographic process.

2.4. Layer-by-layer assembly of sub-monolayer gold-PDDAC films

The layer-by-layer assembly of the gold nanoparticle poly-(diallyldimethylammonium chloride) (PDDAC) films consisted of a sequence of liquid immersion steps with: (i) an aqueous PDDAC solution (3 wt.% in water) for 60 s followed by rinsing with distilled water, (ii) dipping into 20 nm diameter gold colloid (ca. 0.01% in HAuCl, Sigma–Aldrich) for 10 min followed by rinsing with distilled water and drying in air. This completed a single deposition cycle of the gold-PDDAC film. The process was then repeated until the necessary number of layers was achieved. The colour of the deposit is initially red but it turns dark green (see Fig. 1) in subsequent deposition cycles due to gold nanoparticle surface plasmon interactions [22].

3. Results and discussion

3.1. Formation and morphology of sub-monolayer gold nanoparticle-PDDAC assemblies on patterned tin-doped indium oxide (ITO) substrates

The formation of layered structures based on the layer-by-layer deposition of gold nanoparticles with suitable binder systems has been explored in several recent studies [23–25]. Interesting thin film nanocomposite structures with novel

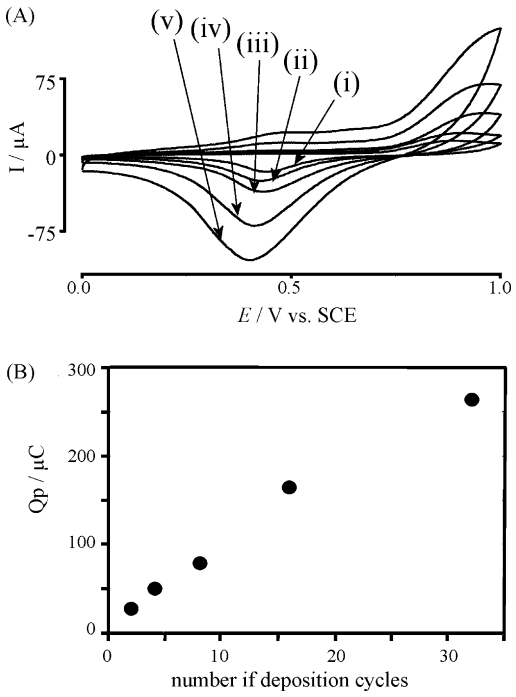

Fig. 2. (A) Cyclic voltammograms (scan rate 0.1 V s^{-1}) for the surface oxidation and re-reduction for a gold-PDDAC modified ITO electrode (area 1 cm^2) with (i) 2, (ii) 4, (iii) 8, (iv) 16, and (v) 32 deposition cycles in aqueous 0.1 M phosphate buffer pH 7.2 (B) Plot of the charge under the voltammetric reduction peak for the gold-PDDAC film as a function of the number of deposition layers.

electronic and electrochemical properties can be obtained [26]. In this report, 20 nm diameter gold nanoparticles are employed and they are bound to a ITO-coated glass substrate with the help of poly-(diallyldimethylammonium chloride) (or PDDAC) in a cyclic aqueous deposition process (see Section 2).

Initially, the gold nanoparticle assembly process is investigated. The formation of the gold film deposit is readily monitored with cyclic voltammetry in aqueous 0.1 M phosphate buffer (pH 7) solution. Under these conditions the gold surface is known to exhibit a surface oxidation response (at ca. 0.8 V vs. SCE) and the associated re-reduction response (at ca. 0.4 V vs. SCE) as shown in Fig. 2. The gold surface signal is observed immediately after the first deposition cycle and in each subsequent deposition cycle the gold surface response is increased (see Fig. 2B). It can be concluded that a highly regular layer-by-layer growth occurs. Under these conditions a planar macroscopic gold surface shows typically a 1 mC cm^{-2} oxidation/re-reduction charge. Therefore from the charge for the 10-layer deposit it can be calculated that approximately 10% electrode coverage has been reached (see plot in Fig. 2B). The colour of the gold coating develops from red in the initial cycle into dark green in subsequent deposition cycles. This colour change is due to the surface plasmon interaction of individual gold nanoparticles [27].

Next, the gold nanoparticle-PDDAC film deposits were investigated by electron microscopy. Fig. 3 confirms the presence of gold nanoparticles of ca. 20 nm diameter. The deposition conditions result in sub-monolayer films of nanoparticles with a density consistent with the estimate obtained from the charge observed in cyclic voltammograms. The approximate surface coverage for the 10-layer deposit (see Fig. 3B) is ca. 5×10^{10} particles cm^{-2}. Perhaps surprisingly, the continued deposition of gold nanoparticles does not lead to a smooth and homogeneous coverage of the surface. Figs. 3B and C clearly demonstrate that cluster formation is preferred and the formation

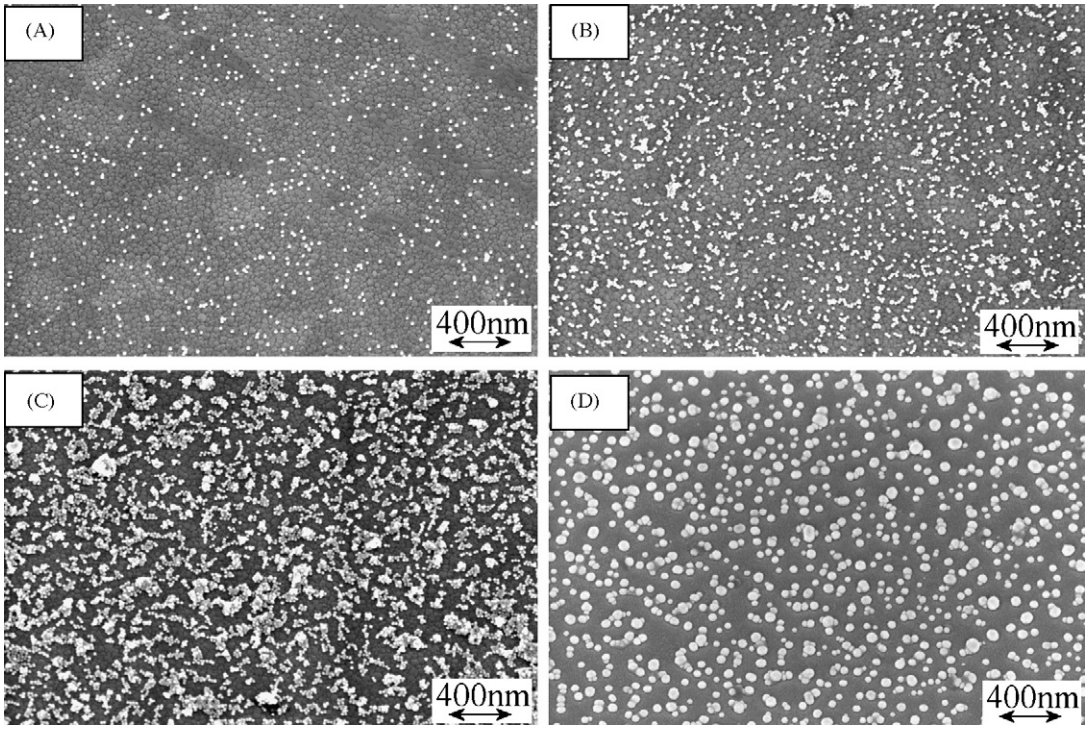

Fig. 3. FEGSEM images of (A) a 1-layer gold-PDDAC film, (B) a 10-layer, (C) a 40-layer gold-PDDAC film, and (D) a 10-layer gold-PDDAC film heat-treated at 500 °C for 30 min.

of interconnecting junctions is very rare. This could be attributed to the deposition process in which PDDAC is more readily adhering to the gold nanoparticles and this may cause a preferential deposition of the next gold nanoparticles onto existing clusters rather than onto the bare ITO surface. However, kinetic or surface morphology effects may also be important.

In order to clean and modify the gold nanoparticle decorated surfaces two strategies were employed and compared. A thermal treatment in air (500 °C for 30 min) which is known to remove all volatile and combustible organic components from the surface [28] and a room temperature UV-ozonolysis process [29] are investigated. The thermal treatment caused a colour change of the gold deposit back to red which is indicative of the presence of individual particles rather than of clusters of gold nanoparticles. Indeed, FEGSEM imaging reveals that partial sintering of gold nanoparticles occurs under these conditions. Fig. 3D shows that individual bigger particles have formed when compared to Fig. 3B (the change in particle size is probably affecting the red coloration when compared to the original 20 nm diameter particles but the analysis of this effect would require more accurate light adsorption measurements which are not reported here). In contrast, a 30 min UV-ozonolysis treatment at room temperature did not cause any colour modification (the cluster morphology remains intact) or any FEGSEM-visible changes in the nanoparticle deposit appearance. FEGSEM images obtained for UV-ozonolysis-treated 10- or 40-layer films are indistinguishable from images shown in Fig. 3B and C and therefore not shown here. It is assumed that the room temperature UV-ozonolysis process only removes organics (by oxidation to volatile oxides) without attacking the inorganic components of the film.

3.2. Electrochemical characterisation of sub-monolayer gold nanoparticle-PDDAC assemblies and ozone treated gold nanoparticle assemblies on patterned tin-doped indium oxide (ITO) substrates

In order to characterize the effect of clustering on the electrical conductivity of gold-PDDAC films a patterned ITO electrode was employed. Fig. 1 shows the design with two ITO fields separated by a 40 μm gap. The gold-PDDAC film was deposited across the gap and conductivity data recorded as a function of film thickness. Fig. 4A shows typical cyclic voltammograms indicating highly resistive behaviour (curve (i)). Thermal treatment of these films resulted in electrically inactive (insulating) films probably due to the spatial separation between individual particles (see Fig. 3D). However, after UV-ozonolysis treatment, well-defined voltammograms are obtained (curve (ii)). The analysis of these data was based on the assumption that the slope in the signal is indicating resistance (given by $\Delta U/\Delta I$). In addition, an apparent capacitive current component is observed (see curve (ii)) which is analysed by calculating the apparent capacitance (given by the capacitive current divided by the scan rate [30]). The reason for the capacitive currents is explained below.

The conductance of gold-PDDAC film deposits was extremely low and not measurable even after up to 40 deposition cycles. However, UV-ozonolysis of the gold nanoparticle

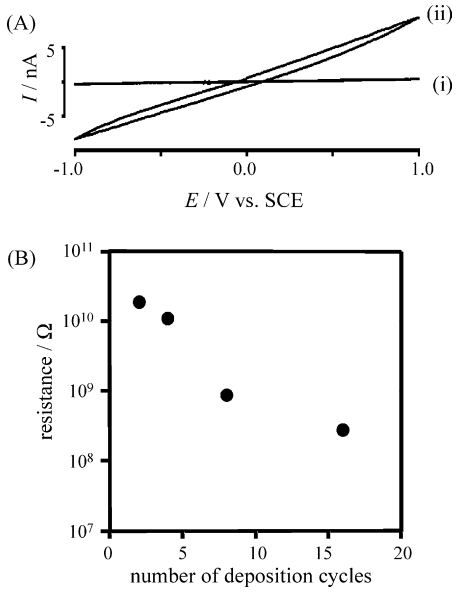

Fig. 4. (A) Cyclic voltammograms (scan rate 0.02 V s^{-1}) obtained for a 16-layer gold-PDDAC film on a 40 μm gap electrode obtained in two-electrode mode. Curve (i) was recorded before and curve (ii) after UV-ozonolysis treatment. (B) Plot of the apparent resistance of gold-PDDAC film deposits as a function of the number of deposition cycles. Data for 0-layer deposit and for gold-PDDAC deposits is much more resistive and not included (see text).

deposit did result in measurable current responses. A plot of the resistance versus the number of deposition cycles is shown in Fig. 4B and it demonstrates an approximately exponential dependence of the resistance on deposition cycles. The reason for this kind of dependence is in part due to electrical conductance in sub-monolayer deposits (vide infra) but also due to ionic conductivity as is shown next.

The conductance measurements for UV-ozonolysis cleaned gold nanoparticle films were repeated and an effect was observed in different environments (ambient air, argon, vacuum, etc.). The conductance was observed to drop significantly under vacuum or dry argon conditions (however, the conductance did not drop to zero) and is therefore particularly sensitive to the level of ambient humidity. It has been shown recently that chemiresistor-type devices can be sensitive to humidity depending on the gold-capping agent and depending on the type of vapour detected [31]. In these devices both resistance and capacitive responses are observed in the presence of elevated humidity levels [32]. Here, a series of experiments was conducted under controlled humidity conditions and results are shown in Fig. 5.

It can be observed that both the conductance of the probe and the apparent capacitive current are strongly humidity dependent and increasing with humidity. The apparent capacitive current is significant at humidity levels higher than 50% and it can be explained with the formation of an extremely thin film of water on the sub-monolayer gold nanoparticle film modified substrate (see Fig. 6). In the conductance data it can be seen that the onset of the "liquid-like" properties (= lateral ion conduction) of the water film occurs at ca. 40% relative humidity. Unfortunately, the chemical nature of the ionic components in the liquid layer is currently not known. The dependency of both capacitance and

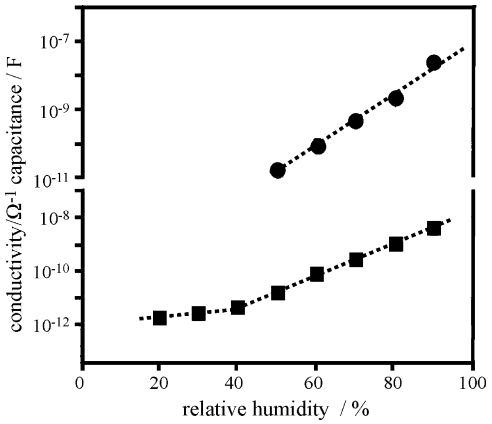

Fig. 5. Plot of the apparent capacitance and conductance (obtained from cyclic voltammograms at a 40 μm ITO gap electrode) of a 16 deposition cycle gold nanoparticle deposit (after UV-ozonolysis) in air with controlled humidity ($T = 20\,^{\circ}C$).

conductance on the humidity are exponential in good approximation. A schematic drawing of the liquid water film formation due to humidity is shown in Fig. 6.

The presence of the liquid water film allows electrical conductivity and capacitive current contributions to be explained. The gold nanoparticle may also contribute to this effect by acting as a scaffold supporting the liquid film. It has to be pointed out that the measured or apparent capacitance is not the real capacitance of the two ITO electrodes but only a fraction of this. The apparent capacitance increase becomes more significant as the thickness of the water film is gradually increasing with relative humidity and this is connected with the water film on the ITO film gradually making a larger electrode area accessible.

3.3. Electrochemical characterisation of sub-monolayer gold nanoparticle assemblies on patterned tin-doped indium oxide (ITO) substrates exposed to dithiol vapours

The electrical conductivity of the gold nanoparticle film deposit after UV-ozonolysis cleaning and in a very dry environment (vacuum, argon) is typically $1.5 \times 10^{-10}\,\Omega^{-1}$ for a 16 deposition cycle gold nanoparticle film. This is two-orders of magnitude lower when compared to the conductivity observed in ambient air (ca. 60% relative humidity). However, this level

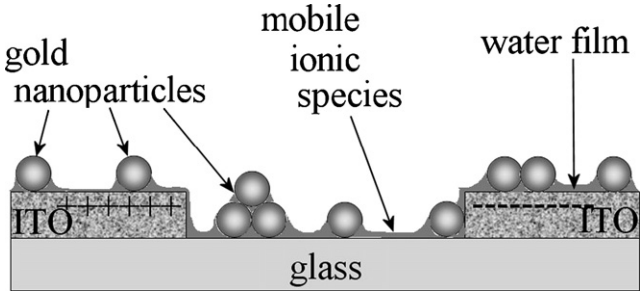

Fig. 6. Schematic drawing of the gold nanoparticle deposit within the ITO gap electrode system and a thin film of water forming an ionically conducting film allowing the charging of the two ITO electrode and therefore allowing a capacitive current component.

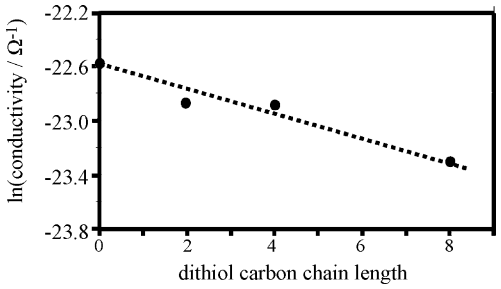

Fig. 7. Plot of the conductance measured for a 16 deposition cycle gold nanoparticle film (UV-ozonolysis cleaned) across a 40 μm gap as a function of the number of carbon atoms in the alkyl chain of dithiols.

of conductivity is significant and also a function of the number of deposition cycles. This residual electrical conductivity is believed to arise from electron tunneling events along random pathways across the 40 μm gap between the two ITO electrodes. In order to explore this finding in more detail the UV-ozonolysis cleaned conductivity probes were exposed to differently contaminated vapour atmospheres. Both thiols and dithiols resulted in immediate and significant changes in electrical conductivity (at 0% humidity) and these changes were reversed after UV-ozonolysis. Below the effect of some dithiols is explored in more detail.

Fig. 7 shows that a systematic decrease in conductance occurs after exposure of the probe to ethylenedithiol, butylenedithiol, and octylenedithiol with an approximately exponential dependency on the number of carbon atoms. Only one probe was employed and UV-ozonolysis cleaned between experiments. The systematic decrease in conductance is consistent with impeded electron tunneling across random junction networks. However, the slope (or decay factor) of the plot in Fig. 7 is inconsistent with the expected behaviour for a single junction (expected slope ca. $0.87\,\text{Å}^{-1}$ [33], observed slope ca. $0.06\,\text{Å}^{-1}$). In order to explain the observed behaviour we speculate that (i) dithiol molecules are able to (at least partially) penetrate into gold–gold contacts (possibly re-filling gaps left behind after removal of PDDAC) thereby changing the tunnel current magnitude and (ii) in a network of junctions the current will flow along the path of lowest resistance and therefore the effect of the dithiol is probably reduced to a statistically averaged value favouring the more conducting junctions. It is unlikely that all junctions are fully responsive (fully covered in dithiol) and therefore the slope is reduced. Other explanations of the observed data could be based on the effect of the thiol adsorption onto the gold surface on electrical conductivity and further work will be required to explore these effects in more detail.

4. Conclusions

The early stages of the formation of a tunnel junction network between two ITO electrodes with a 40 μm gap have been investigated. The layer-by-layer deposition process allows gold nanoparticles to be assembled and the resistivity of the resulting probe to be tuned. The electrical properties of the probe after UV-ozonolysis cleaning have been demonstrated to depend on

humidity and on specific adsorption from the gas phase onto the gold particles. In future, this kind of probe could offer low cost and highly versatile sensor films.

Acknowledgement

R.W.F. thanks the Innovative Electronic Manufacturing Research Council (IeMRC) for a studentship.

References

[1] W.P. McConnell, J.P. Novak, L.C. Brousseau, R.R. Fuierer, R.C. Tenent, D.L. Feldheim, Electronic and optical properties of chemically modified metal nanoparticles and molecularly bridged nanoparticle arrays, J. Phys. Chem. B 104 (2000) 8925–8930.
[2] L. Han, D.R. Daniel, M.M. Maye, C.J. Zhong, Core-shell nanostructured nanoparticle films as chemically sensitive interfaces, Anal. Chem. 73 (2001) 4441–4449.
[3] S.D. Evans, S.R. Johnson, Y.L.L. Cheng, T.H. Shen, Vapour sensing using hybrid organic–inorganic nanostructured materials, J. Mater. Chem. 10 (2000) 183–188.
[4] H. Wohltjen, A.W. Snow, Colloidal metal–insulator–metal ensemble chemiresistor sensor, Anal. Chem. 70 (1998) 2856–2859.
[5] W.P. Wuelfing, R.W. Murray, Electron hopping through films of arenethiolate monolayer—protected gold clusters, J. Phys. Chem. B 106 (2002) 3139–3145.
[6] J.P. Choi, M.M. Coble, M.R. Branham, J.M. DeSimone, R.W. Murray, Dynamics of CO_2-plasticized electron transport in Au nanoparticle films: opposing effects of tunneling distance and local site mobility, J. Phys. Chem. C 111 (2007) 3778–3785.
[7] F.N. Crespilho, F.C. Nart, O.N. Oliveira, C.M.A. Brett, Oxygen reduction and diffusion in electroactive nanostructured membranes (ENM) using a layer-by-layer dendrimer-gold nanoparticle approach, Electrochim. Acta 52 (2007) 4649–4653.
[8] A. Escorcia, A.A. Dhirani, Electrochemical properties of ferrocenylalkane dithiol-gold nanoparticle films prepared by layer-by-layer self-assembly, J. Electroanal. Chem. 601 (2007) 260–268.
[9] Y. Joseph, B. Guse, A. Yasuda, T. Vossmeyer, Chemiresistor coatings from Pt- and Au-nanoparticle/nonanedithiol films: sensitivity to gases and solvent vapors, Sens. Actuators B: Chem. 98 (2004) 188–195.
[10] W. Zhao, J.J. Xu, H.Y. Chen, Extended-range glucose biosensor via layer-by-layer assembly incorporating gold nanoparticles, Front. Biosci. 10 (2005) 1060–1069.
[11] A. Singh, S. Hede, M. Sastry, Spider silk as an active scaffold in the assembly of gold nanoparticles and application of the gold–silk bioconjugate in vapor sensing, Small 3 (2007) 466–473.
[12] Y. Joseph, N. Krasteva, I. Besnard, B. Guse, M. Rosenberger, U. Wild, A. Knop-Gericke, R. Schlogl, R. Krustev, A. Yasuda, T. Vossmeyer, Gold-nanoparticle/organic linker films: self-assembly, electronic and structural characterisation, composition and vapour sensitivity, Faraday Discus. 125 (2004) 77–97.
[13] N. Krasteva, Y. Fogel, R.E. Bauer, K. Mullen, N. Matsuzawa, A. Yasuda, T. Vossmeyer, Vapor sorption and electrical response of Au-nanoparticle-dendrimer composites, Adv. Funct. Mater. 17 (2007) 881–888.
[14] M.C. Leopold, R.L. Donkers, D. Georganopoulou, M. Fisher, F.P. Zamborini, R.W. Murray, Growth, conductivity, and vapor response properties of metal ion-carboxylate linked nanoparticle films, Faraday Discus. 125 (2004) 63–76.
[15] W.R. Yang, J.J. Gooding, Z.C. He, Q. Li, G.N. Chen, Fast colorimetric detection of copper ions using L-cysteine functionalized gold nanoparticles, J. Nanosci. Nanotechnol. 7 (2007) 712–716.
[16] Z.H. Zhong, D.L. Wang, Y. Cui, M.W. Bockrath, C.M. Lieber, Nanowire crossbar arrays as address decoders for integrated nanosystems, Science 302 (2003) 1377–1379.
[17] R.L. McCreery, Molecular electronic junctions, Chem. Mater. 16 (2004) 4477–4496.
[18] A. Troisi, M.A. Ratner, Molecular signatures in the transport properties of molecular wire junctions: what makes a junction "molecular"? Small 2 (2006) 172–181.
[19] A. Kolmakov, M. Moskovits, Chemical sensing and catalysis by one-dimensional metal-oxide nanostructures, Ann. Rev. Mater. Res. 34 (2004) 151–180.
[20] D.R. Lide (Ed.), CRC Handbook of Chemistry and Physics, 74th edition, CRC Press, London, 1993–1994, pp. 15–25.
[21] T.H. Tsai, Y.F. Wu, Organic acid mixing to improve ITO film etching in flat panel display manufacturing, J. Electrochem. Soc. 153 (2006) C86–C90.
[22] Z.Y. Zhong, K.B. Male, J.H.T. Luong, Plasmon More recent progress in the preparation of Au nanostructures, properties, and applications, Anal. Lett. 36 (2003) 3097–3118.
[23] K.J. McKenzie, F. Marken, Accumulation and reactivity of the redox protein cytochrome c in mesoporous films of TiO_2 phytate, Langmuir 19 (2003) 4327–4331.
[24] E.V. Milsom, H.R. Perrott, L.M. Peter, F. Marken, Redox processes in mesoporous oxide membranes: layered TiO_2 phytate and TiO_2 flavin adenine dinucleotide films, Langmuir 21 (2005) 9482–9487.
[25] M. Amiri, S. Shahrokhian, F. Marken, Ultrathin carbon nanoparticle composite film electrodes: distinguishing dopamine and ascorbate, Electroanalysis 19 (2007) 1032–1038.
[26] E.V. Milsom, J. Novak, M. Oyama, F. Marken, Electrocatalytic oxidation of nitric oxide at TiO_2–Au nanocomposite film electrodes, Electrochem. Commun. 9 (2007) 436–442.
[27] K.C. Grabar, R.G. Freeman, M.B. Hommer, M.J. Natani, Preparation and characterization of Au colloid monolayers, Anal. Chem. 67 (1995) 735–743.
[28] E.V. Milsom, J. Novak, S.J. Green, X.H. Zhang, S.J. Stott, R.J. Mortimer, K. Edler, F. Marken, Thermal treatment Layer-by-layer deposition of open-pore mesoporous TiO_2-Nafion film electrodes, J. Solid State Electrochem. 11 (2007) 1109–1117.
[29] T. Goto, H. Inokawa, M. Nagase, Y. Ono, K. Sumitomo, K. Torimitsu, Ozonolysis junction cleaning Effect of UV/ozone treatment on nanogap electrodes for molecular devices, Jpn. J. Appl. Phys. 46 (2007) 1731–1733.
[30] F. Scholz (Ed.), Electroanalytical Methods, Springer, Berlin, 2005, p. 38.
[31] P.F. Pang, J.L. Guo, S.H. Wu, Q.Y. Cai, Humidity effect on the dithiol-linked gold nanoparticles interfaced chemiresistor sensor for VOCs analysis, Sens. Actuators B: Chem. 114 (2006) 799–803.
[32] P.F. Pang, Z.D. Guo, Q.Y. Cai, Humidity effect on the monolayer-protected gold nanoparticles coated chemiresistor sensor for VOCs analysis, Talanta 65 (2005) 1343–1348.
[33] E. Tran, C. Grave, G.M. Whitesides, M.A. Rampi, Controlling the electron transfer mechanism in metal-molecules-metal junctions, Electrochim. Acta 50 (2005) 4850–4856.

Biographies

Robert W. French completed a degree in natural sciences in 2006 and is now working as a postgraduate student at the Department of Chemistry at the University of Bath.

Elizabeth V. Milsom obtained her chemistry degree in 2005 and is now completing her PhD in the Department of Chemistry at the University of Bath.

Andriy V. Moskalenko received his PhD degree in 2002 at ILTPE Kharkiv and is now working as postdoctoral researcher in the Department of Physics at the University of Bath.

Sergey N. Gordeev obtained his PhD degree in physics and mathematics in 1983 at Moscow State University and is now working as a senior lecturer in the Department of Physics at the University of Bath.

Frank Marken received his PhD in 1992 at the RWTH Aachen and is now working as a senior lecturer at the Department of Chemistry at the University of Bath.